Available online at www.sciencedirect.com

ScienceDirect

Ciência & Tecnologia dos MATERIAIS

http://ees.elsevier.com/ctmat

Ciência & Tecnologia dos Materiais 29 (2017) 28–38

Investigations on the structure – property relationships of PCGTA welds involving Inconel 718 and AISI 430

K. Devendranath Ramkumar*, T. Harsha Mohan, Rachit Pandey, Vimal Saxena, S. Aravind, Shubham Singh

School of Mechanical Engineering, VIT University, Vellore - 632014, India

Abstract

The present investigation deals with the weldability, structure – property relationship of dissimilar metallurgical joints involving Nickel based superalloy Inconel 718 and ferritic stainless steel AISI 430 using pulsed current gas tungsten welding (PCGTAW) process employing ER2553 and ERNiCrMo-4 filler wires. NDT analysis and macrostructure examination corroborated for defect free weldments. Microstructure studies revealed the presence of unmixed zone at the weld interface of Inconel 718 whereas grain coarsening effect was observed at the heat effected zone (HAZ) of AISI 430. Both cellular and equiaxed dendrites were dominated at the fusion zone of ERNiCrMo-4 weldment; whereas different types of ferrite morphologies such as delta and widmanstätten ferrite were observed at the cap and middle zones of ER2553 fusion zone respectively. It was opined that the tensile failures occurred at the parent metal of AISI 430 for both the fillers. Charpy V-notch studies showed that ERNiCrMo-4 weldment exhibited better impact toughness than ER2553 weldment. Similarly the bend test also recommended the use of ERNiCrMo-4 filler due to the acquaintance of excellent bending strength and soundness. This study also addressed the structure – property relationships of these weldments. The outcomes of the study would be highly beneficial to the nuclear, aerospace and petrochemical industries.

Keywords: nickel based super-alloy; ferritic stainless steel; pulsed current gas tungsten arc welding; structure – property relationship.

1. Introduction

Joining of dissimilar materials has progressed significantly in the recent past owing to their accrued demand in aerospace, nuclear, chemical and thermal power plants. The assortment and application of the dissimilar joints are directed by the in-service requirement wherein involvement of each material is localized for the optimal utilization of their properties, economic feasibility of the materials and ease of fabrication.

Inconel 718, a precipitation hardened Ni based superalloy, finds its application in high temperature stringent operating conditions. Even though high Ni content imparts the required thermo-mechanical properties to sustain stringent environment, this super alloy isn't an economically feasible option while operating at lower risk conditions. Hence a low cost alloy, AISI 430 can be employed at low risk zones to alleviate the cost. AISI 430 is the most used ferritic grade stainless steel as reported by International Stainless Steel Forum (ISSF) [1] which can be used at elevated temperatures. AISI 430 is a medium chromium ferritic stainless steel with a probable chance of grain boundary martensite (GBM) formation during solidification [2]. The presence of grain boundary martensite at the fusion zone was believed to impoverish the impact toughness. It was reported that the addition of Ti or Nb prevents the formation of GMB as both the elements act as delta-ferrite stabilizer suppressing formation of austenite [3]. On the other hand, Hayden et al. [4] and Wright et al. [5] reported that the duplex ferritic-martensitic microstructure formed while welding has greater impact toughness relative to fully martensitic or fully ferritic steels. Due to low carbon content in this steel,

* Corresponding author.

E-mail address: ramdevendranath@gmail.com (K.D. Ramkumar)

http://dx.doi.org/10.1016/j.ctmat.2016.05.005

the martensite formed would be softer compared to high carbon martensite and is known as plate martensite [6]. Also ferritic stainless steels have lower coefficient of thermal expansion and higher thermal conductivity than the austenitic stainless steel and can be advantageous when cyclic temperature resistance is obligatory as reported by Sedricks [7]. Several researchers [2, 8] have addressed the problem related to solidification and liquation cracking during the welding of Nickel based alloys. It was reported by Dupont et al. [8] the susceptibility of solidification and liquation cracking increases due to the formation of Nb precipitates (Ni_3Nb) which segregate into the inter-dendritic region thereby decreasing the solidus temperature. Similar problems were also reported by Odabasi et al. [9] during laser welding of Inconel 718. As reported by various researchers [10-12], the formation of laves phase in the fusion zone as well as in the HAZ of Inconel 718 had detrimental effect on the weld mechanical properties. Also the presence of this laves phase serve as the notable sites for easy crack initiation and propagation which affects the mechanical properties such as tensile and rupture properties, ductility, fracture toughness and fatigue life of the welded component.

Radha Krishna and Prasad Rao [13] proposed various methods of controlling the laves phase formation by the use of (a) current pulsing technique (b) low Nb fillers (c) faster cooling rate (d) heat extraction technique (e) steep thermal gradients and (f) electron beam oscillation techniques. Pulsed current gas tungsten arc welding (PCGTAW) is an extensively used welding technique and has several advantages over the conventional arc welding process. Several researchers [14-16] experimented using PCGTAW and all reported that the use of pulsed current technique significantly improved the metallurgical and mechanical properties of the weld.

Devendranath et al. [12] investigated the continuous and pulsed current GTA welding of Inconel 718 and AISI 316L using ER2553 and ERNiCu-7. The authors reported that these fillers were effective in controlling laves phase. Farahani et al. [16] compared the microstructure and impact strength of continuous current gas tungsten arc (CCGTA) and PCGTA weldments of alloy 617. The authors reported that the impact toughness was better for the PCGTA weldment due to the grain refinement.

It is often witnessed that the ductility and toughness of weldments of ferritic stainless steels are adversely affected by the grain coarsening in both weld and HAZ occasioned by the absence of phase transformation during solidification to room temperature as reported by Pickering [17] and Kou Sindo [18]. Alizadeh [19] performed resistance spot welding of AISI 430 and the author observed the formation of ferrite- martensite dual microstructure in the medium temperature HAZ with the highest hardness being in that region. Dissimilar friction welding of austenitic and ferritic stainless steel has been performed by Sathyanarayana et al. [20], the work cited that the weldments offered better toughness and strength relative to the ferritic base metal.

Dissimilar welding of nickel based alloys and ferritic stainless steel faces certain challenges such as formation of cracks at the interface, abrupt variation in hardness close to weld zone occasioned by their difference in coefficient of thermal expansion (CTE) which might result in in-service failure. It is evident from these works [12,20,21] that prime focus was laid on bimetallic joints of Nickel based alloy and austenitic grade stainless steels. Ferritic grade stainless steel on the other hand offers comparable mechanical properties, relatively better stress corrosion cracking resistance and low cost as compared to austenitic grade stainless steel. Adding to this AISI 430 is relatively less susceptible to weld solidification cracking compared to AISI 304 [2]. Despite ferritic stainless steel's aforementioned properties, they are seldom used in dissimilar combinations with Ni based alloys. Hence a study is required to assess the microstructure changes and the corresponding effects in the mechanical properties during the PCGTA welding of Inconel 718 and AISI 430. In this research article, an attempt has been made to achieve the dissimilar combination of Inconel 718 and ferritic stainless steel AISI 430 using pulsed current gas tungsten arc welding (PCGTAW) employing ER2553 and ERNiCrMo-4 filler metals. A detailed structure-property relationship has been carried out to underline the potential of the dissimilar joint.

2. Experimental

2.1. Base metals and welding procedure

The chemical compositions of the base metal and that of consumables were ascertained by dry spectroscopic method and are enlisted in Table 1.

Table 1. Chemical composition of base and filler metals.

Chemical composition (% by weight)										
Base/Filler	C	Si	Mn	Cr	Ni	Nb	Mo	Fe	Cu	Other elements
Inconel 718	0.031	0.1	0.2	17.69	Bal.	4.9	2.9	20.07	0.11	P – 0.09; Al – 0.29; Ti – 0.72; Co – 0.360; S – 0.012;
AISI 430	0.048	0.376	0.319	16.24	---	---	---	Bal.	---	P – 0.025; S – 0.005;
ER2553	0.04	1.0	1.5	25.5	5.5	---	3.4	Bal.	2.0	P – 0.04; S – 0.03; N – 0.175;
ERNiCrMo -4	0.02	0.030	0.510	15.90	Bal.	---	16.25	5.45	0.05	P – 0.007; S – 0.003; Al- 0.31; Ti – 0.10; Co – 0.36; V- 0.18; W-3.4

The as-received base metals employed in the study were solution annealed Inconel 718 and hot rolled AISI 430 stainless steel plates of thickness 5 mm, which were dimensioned to 170 mm × 55mm × 5mm prior to welding using Wire cut Electric Discharge Machining (WEDM) process. Both super duplex stainless steel (ER2553) and Inco-weld – C276 (ERNiCrMo-4) consumables were used for welding.

Mechanical and chemical polishing were employed prior to welding to ensure the specimens are free from any contamination. All the welding experiments were carried out using Kempi Master TIG welding equipment using pulsed current mode. Standard V-groove butt configurations with an included angle of 70º, root gap of 2 mm and a size land of 1 mm were employed for the experiments. A copper back plate welding fixture was used to facilitate the dissipation of heat and provide rigidity and adequate grip to circumvent distortion and bending. The diameter of the fillers employed in the study is 2.4 mm.

Constant argon purging was provided at a rate of 15 lpm during welding to prevent the inclusion of N_2, O_2, and H_2 into the weld zone which deteriorates the properties of the joint. Due to the scarce information available in the literature for selecting the welding parameters, the parameters were established based on bead on plate welding and also by the trail runs and the finalized parameters are shown in Table 2.

2.2. Metallurgical and mechanical characterization of dissimilar weldments

After welding, the bimetallic joints were subjected to both dye-penetrant and gamma ray Non-destructive Testing (NDT) techniques to ensure for surface or sub-surface flaws. Further, the welded specimens were cut as per the ASTM standards to conduct various metallurgical and mechanical tests to arrive out at the structure – property relationships. Microstructure examination and hardness measurements were carried out on the cross-sectioned coupons dimensioned 28 mm × 10mm × 5mm, covering all the zones of the weldment vis-à-vis HAZs of both the metals, parent metals, and weld zone, termed as "composite zones". Standard metallographic procedures including polishing using SiC emery sheets of grits size papers ranging from 220 to 1000 followed by disc polishing using diamond paste and aerosol as lubricant were carried out on the composite coupons to obtain mirror like finish of 1µm. Microstructure studies were carried out using both optical microscopy (OM) and scanning electron microscopy (SEM) techniques. Electrolytic etching using 10% Oxalic acid [6 V DC supply; current density of 1 A/cm^2; 30 s] was employed to reveal the microstructure. Following microstructure analyses, the mechanical properties of the weldments were investigated by subjecting the weldments to various tests. Tensile specimens were prepared as per ASTM E8/8M standard and the test was conducted using Instron Universal Testing Machine with a cross-head velocity of 2 mm/min to produce a strain rate of 3.3×10^{-4} s^{-1} which is well in the range as prescribed by ASM International handbook of Mechanical Testing and Evaluation. Charpy V-notch test was conducted as per ASTM E23 – 12C standard on sub-sized specimens (55 mm × 10 mm × 5mm). The impact load was directed to the weld zone with the notch to induce fracture at the weld zone and to study its strength. Micro-hardness examinations with a standard load of 500gf and a dwell time of 10s were carried out on the composite regions of the weldments vis-à-vis cap, filler, and root passes with a regular interval of 0.25 mm. Furthermore, to determine the soundness and ductility of the weldments, bend test was carried on the coupons having dimensions of 152 mm × 38 mm × 4 mm as per the ASTM: E190-92 standard. To ascertain the mode of fracture during tensile and impact test, SEM analysis was carried out on the fractured samples. The samples were cleaned ultrasonically before the images were captured. The following sections deal with the results and discussion of the experimental work.

Table 2. PCGTA welding parameters.

Filler wire	No. of pass	Current (A)		Voltage (V)	Frequency (HZ)	Duty Cycle	Cumulative Heat Input (kW/mm)
		Peak current	Background current				
ER2553	Root	180	90	11.94	8	50	1.716
	Filler Pass 1	180	90	12.1			
	Filler Pass 2	180	90	13.07			
	Cap	180	90	12.62			
ERNiCrMo-4	Root	180	90	11.31	8	50	1.669
	Filler Pass 1	180	90	11.42			
	Filler Pass 2	180	90	12.2			
	Cap	180	90	12.05			

3. Results and discussion

3.1. Candidate metals

The as-received Inconel 718 was observed to have coarse austenitic grains as its microstructure and AISI 430 had a fully ferritic microstructure with carbide inclusions as depicted in Fig. 1. The ultimate tensile strength and 0.2% proof strength of Inconel 718 alloy was found to be 763 MPa and that of AISI 430 was 516 Mpa respectively. The average impact toughness of the base metals was observed to be 12 J for AISI 430 and 77 J for Inconel 718.

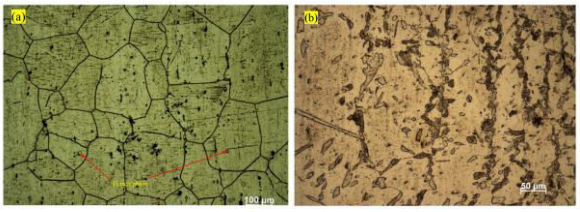

Fig. 1. Microstructure of the base metals showing (a) Inconel 718 and (b) AISI 430.

3.2. Microstructure examination

3.2.1. ER2553 weldment

Microstructure examination at the HAZ of Inconel 718 (Fig. 2a) showed the presence of unmixed or partially melted zone with the formation of secondary phases. This could be due to the notable differences in the chemical composition of the filler and Inconel 718. Similarly the grain coarsening effect observed at the HAZ of AISI 430 could be attributed to the higher heat inputs emerged during multi-pass welding (Fig. 2b). SEM and Energy Dispersive X-ray Analysis (EDAX) point analysis shown in Fig. 3, depicted the presence of tiny and shiny, white phases as precipitates.

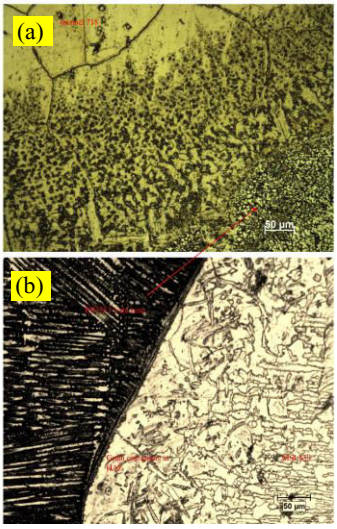

Fig. 2. Interface microstructure of (a) Inconel side (b) AISI 430 side of the weldment employing ER2553 filler.

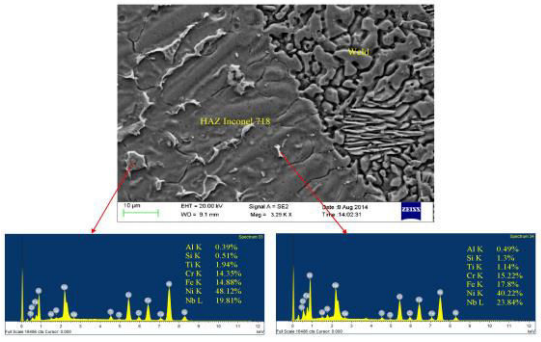

Fig. 3. SEM/EDAX point analysis at the interface of Inconel 718 employing ER2553 filler.

These conspicuous shiny phases were enriched in Nb, Cr and Fe and depleted with Ni. This could be probably Ni_3Nb, Nb rich eutectics and/or Laves phase. Apart from grain coarsening effect, the formation of grain boundary martensite was witnessed along the coarsened boundaries. This could be attributed to lack of ferrite stabilizing agents despite a low level of carbon content. [3]. It could also be reasoned to the number of passes employed in the welding. As reported by Chih-Chun Hsieh et al. [23], the formation tendency of α'-martensite in recrystallized δ-ferrite grains increases as the welding pass number increased from 1 to 3. SEM/EDAX point analysis at the fusion zone adjacent to AISI 430 is shown in Fig. 4.

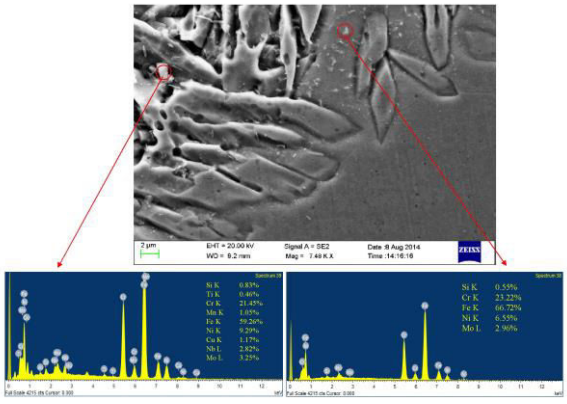

Fig. 4. SEM/EDAX point analysis at the interface of AISI 430 employing ER2553 filler.

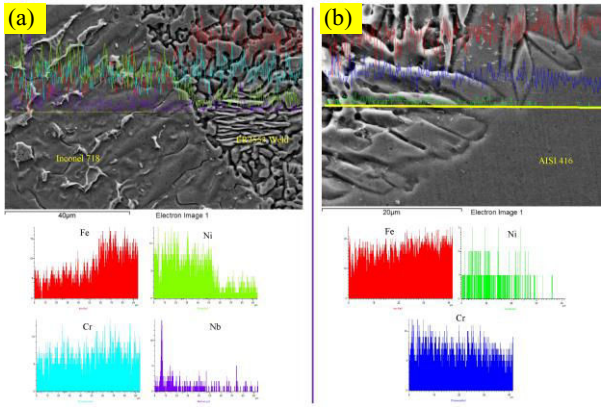

Fig. 5. Line mapping analysis at the weld interface of (a) Inconel 718 and (b) AISI 430 respectively using ER2553 filler.

Scarce, tiny Nb, Mo rich phases were entangled at the dendritic arms of the fusion zone despite ER2553 and AISI 430 having no Nb content implying that Nb has moved from Inconel 718. Due to the higher melting point of ER2553, the AISI 430 must have been liquated for a longer time facilitating the above migration process. This elemental movement could also be possible due to the multi-pass welding. Also the presence of Ni was observed at the weld interface of AISI 430. Although the base metal AISI 430 has no Ni content in it, the Ni could have diffused from the weld zone as well as from Inconel 718 to AISI 430. This could be well understood from the EDAX line mapping analysis at the weld interface of AISI 430 and Inconel 718 is shown in Fig. 5.

Fig. 6 shows the microstructure of the fusion zone containing the typical ferrite morphologies such as vermicular δ ferrite at the cap and the formation of acicular and widmanstätten ferrite along with austenite at the middle and root passes while employing ER2553 filler. The acicular and Widmanstätten ferrite formation at the fusion zone was also favoured due to the presence of Nb which migrated from the Inconel 718 to the fusion zone during welding. This is well in agreement with the studies of Bodnar and Hansen [24].

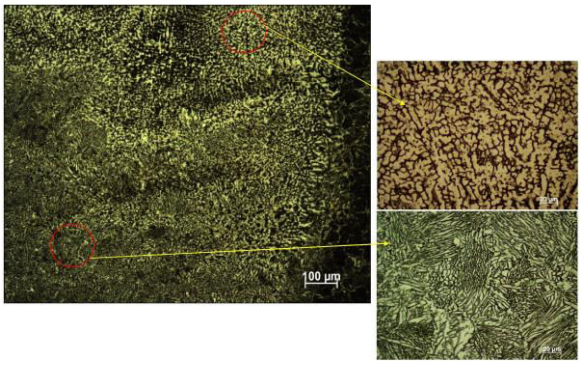

Fig. 6. Fusion zone microstructure of ER2553 weldment showing delta ferrite stringers and Widmanstätten ferrite in the austenite network.

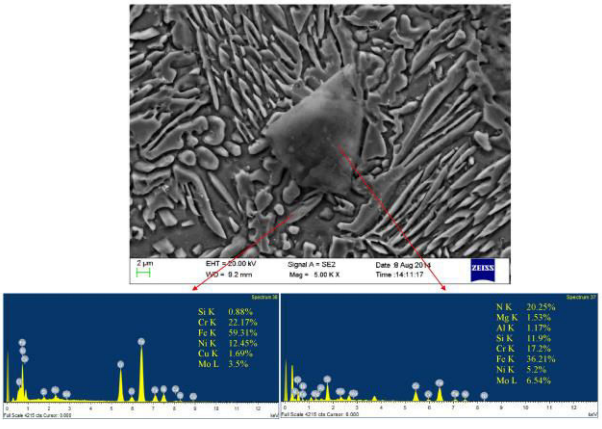

Fig. 7. SEM/EDAX point analysis at the fusion zone employing ER2553 filler.

The authors reported that the higher levels of Nb and Mn had the greatest propensity for Widmanstätten structure formation. The formation of delta ferrite at the cap zone could be attributed to the faster cooling experienced in the cap pass. SEM/EDAX point analysis shown in Fig. 7 inferred the presence of Ni, Mo rich side plates of Widmanstätten austenite.

The scarcely available conspicuous phases appearing in the fusion zone were enriched with Fe, Cr, Si and N. However the Cr_2N formation could be confirmed only by Transmission Electron Microscopy (TEM) analysis which is not reported in the current study.

Line mapping analysis was carried out to infer the elemental movement at the fusion zone and the result is shown in Fig. 8. It is well inferred from the line mapping analysis that the Ni content is varying between the austenite and ferrite.

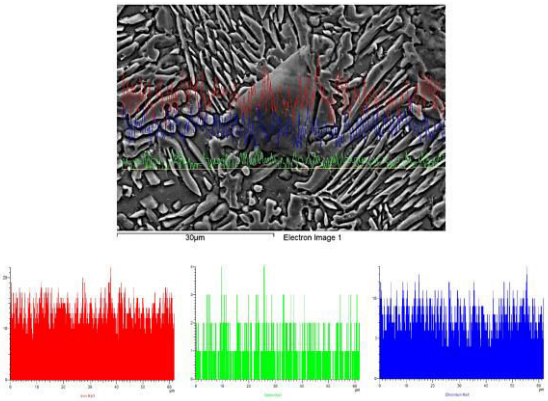

Fig. 8. EDAX line mapping analysis at the fusion zone of ER2553 weldment.

3.2.2. ERNiCrMo-4 weldment

The microstructural examination at the weld interface of ERNiCrMo-4 weldment is shown in Fig. 9. The formation of secondary phases was witnessed at the HAZ of Inconel 718 (Fig. 9a). Similarly a slight grain coarsening effect was observed at the HAZ of AISI 430 (Fig. 9b). This could be observed due to the effect of multi-pass welding and the slow cooling rates developed due to the same.

As discussed in section 3.2.1, the shiny conspicuous phases enriched with Nb, Mo were observed at the HAZ of Inconel 718 (Fig. 10) as well as the weld interface. Whereas, the weld zone adjacent to AISI 430, the tiny phases appearing white in color were enriched with Mo and W. This could be due to the presence of these elements in the filler wire (Fig. 11). The line mapping analysis shown in Fig. 11a also confirmed that these secondary phases were enriched with Nb content.

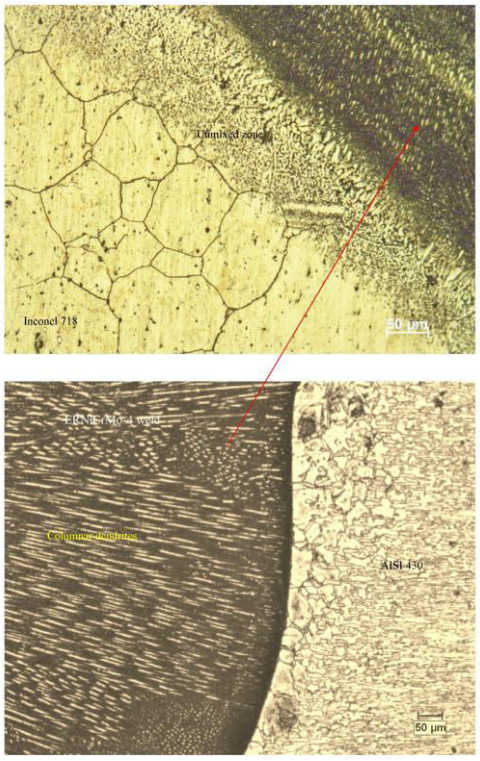

Fig. 9. Interface microstructure of (a) Inconel side (b) AISI 430 side of the weldment employing ERNiCrMo-4 filler.

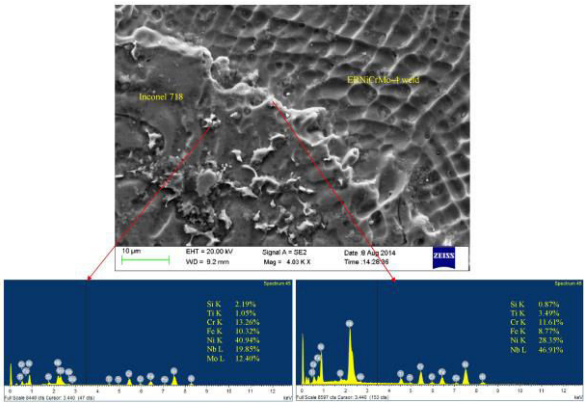

Fig. 10. SEM/EDAX point analysis at the interface of Inconel 718 employing ERNiCrMo-4 filler.

This could be probably the Nb rich eutectics, Ni_3Nb or Laves phase. Fig. 11b shows the line mapping analysis at the interface of AISI 430. It was inferred that Fe had migrated from AISI 430 to the fusion zone; whereas Mo and Ni slightly moved from the fusion zone to AISI 430. This could be attributed to the elemental migration from higher to lower concentrations.

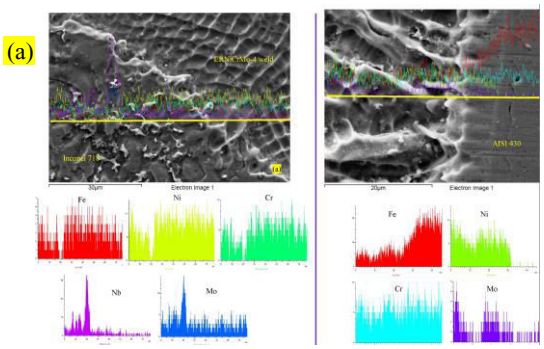

Fig. 11. Line mapping analysis at the weld interface of (a) Inconel 718 and (b) AISI 430 respectively using ER2553 filler.

The fusion zone microstructure consists of well-defined cellular and equiaxed dendrites at the middle pass of the weldment (Fig. 12). Short columnar dendrites were also observed at the fusion zone adjacent to the weld interface of both the metals. This formation of different grains could be attributed to the effect of multi-pass welding and differences in cooling rates across the different passes. The finer equiaxed grain growth witnessed at the fusion zone shall be reasoned out to the effect of pulsed current where the currents were fluctuating between high and low pulses which in turn causes melting and solidification. While performing multi-pass welding, the coarser grains will recrystallize and result in finer grains.

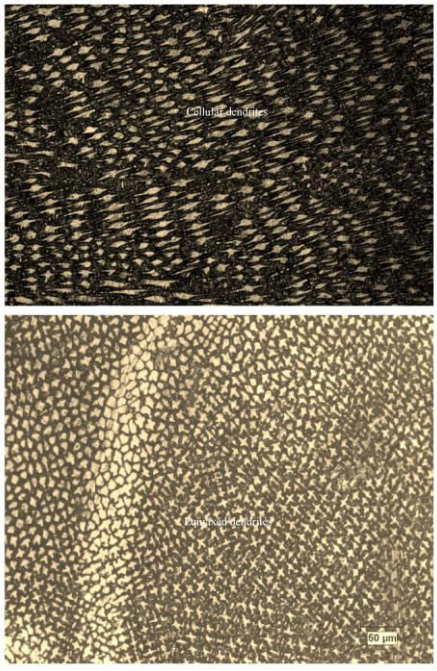

Fig. 12. (a) Cellular dendritic growth and (b) equiaxed dendrites at the fusion zone of ERNiCrMo-4 filler weldment.

Similar observations were reported elsewhere [16, 25, 26]. SEM/EDAX point analysis shows the fusion zone containing the columnar dendrites with the inter-dendritic arms. It is noticed that the Mo and W rich phases were found to be more at the inter-dendritic arms and the matrix was depleted with Mo (Fig. 13). The line mapping analysis at the fusion zone clearly corroborate the presence of tiny, Mo rich phases at the inter-dendritic arms (Fig. 14) which could be attributed to the slower cooling rates developed in arc welding processes.

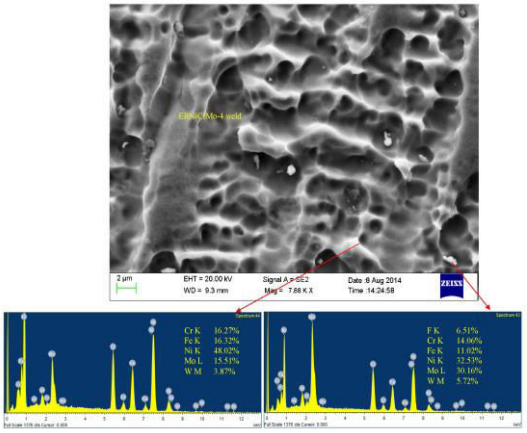

Fig. 13. SEM/EDAX point analysis at the fusion zone employing ERNiCrMo-4 filler.

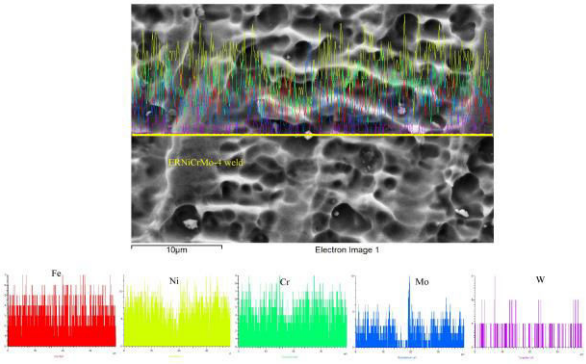

Fig. 14. EDAX line mapping analysis at the fusion zone of ERNiCrMo-4 weldment.

3.3. Mechanical characterization of dissimilar weldments

3.3.1. Hardness measurement

Hardness measurements were recorded for the different passes of the weld vis-à-vis cap, filler, and root passes for both the cases.

Table 3. Average hardness of the weldments.

Description	ER2553 weldment				ERNiCrMo-4 weldment			
	Cap	Middle	Root	Average	Cap	Middle	Root	Average
Average hardness of the weld zone	295	236	249	263	230	234	236	234
Average hardness of the weldment	247	217	217	227	212	207	202	207

It was observed from the hardness profile shown in Fig. 15a that the average hardness value at the weld zone was higher for ER2553 filler (263 HV) than the ERNiCrMo-4 filler (234 HV). Amongst the various passes, the cap zone of ER2553 weldment acquainted for greater average hardness of 295 HV, which might be attributed to the presence of abundance of vermicular delta ferrite. As reported by various researchers, the presence of delta ferrite not only improves the hardness but also improves the hot cracking resistance. Also the delta ferrite has low coefficient of thermal expansion which is helpful in reducing shrinkage stresses in welds. In case of ERNiCrMo-4 weldment, the average hardness at the root pass of the fusion zone was observed to have higher hardness (Fig. 15b). This could be reasoned out to the grain refinement which was facilitated due to reheating actions of this zone due to multi-pass welding.

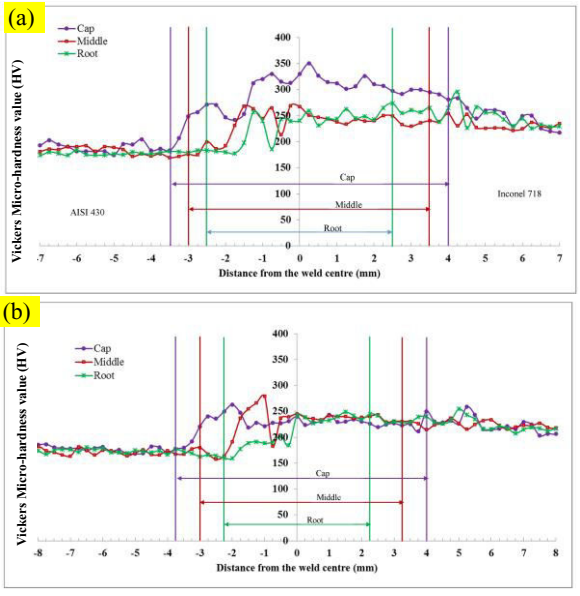

Fig. 15. (a) Hardness profile of the PCGTA weldment of Inconel 718 and AISI 430 employing ER2553 filler (b) Hardness profile of the PCGTA weldment of Inconel 718 and AISI 430 employing ERNiCrMo-4 filler.

Compared to the parent metal of AISI 430, the HAZs of AISI 430 for both the weldments showed a marginal increase in the hardness values such as 235 HV for ER2553 and 226 for ERNiCrMo-4 weldments. As evident from the microstructural examination, the HAZ of the AISI 430 in both the cases was observed to have grain boundary martensite in the ferrite matrix. Hence the hardness studies are in agreement with the microstructural studies. The comparative, average hardness of both the weldments is listed in Table 3.

3.3.2. Tensile test

Tensile test was performed on these dissimilar weldments in order to analyze the response of weldments towards gradually increasing load. As evident from the literature, the AISI 430 is susceptible to grain coarsening at the HAZ hinting that the tensile failure is likely to happen at that region. But in all the tests it was evident that the failure took place in the base metal of AISI 430 (Fig. 16).

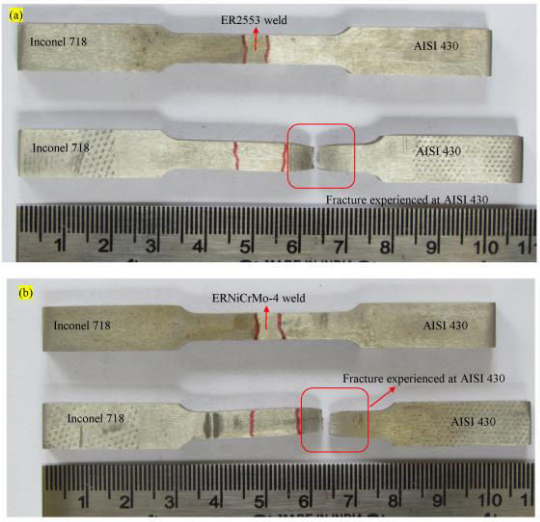

Fig. 16. Tensile tested samples of PCGTA weldment of Inconel 718 and AISI 430 employing (a) ER2553 and (b) ERNiCrMo-4 filler.

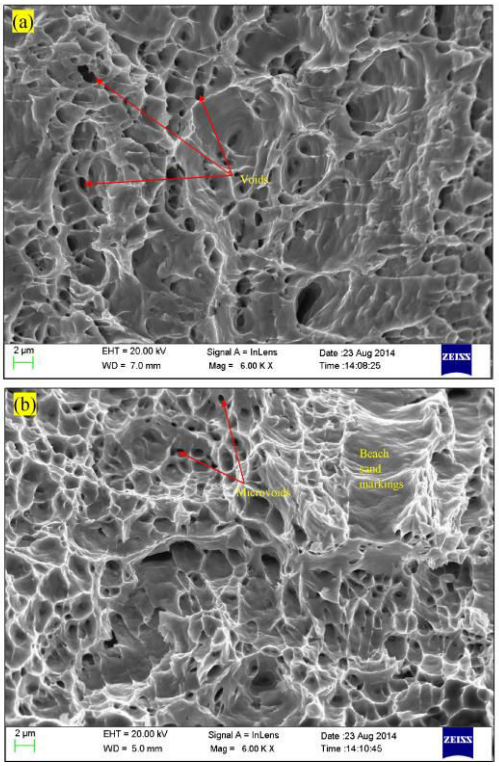

Fig. 17. SEM fractographs on the tensile tested samples of (a) ER 2553 (b) ERNiCrMo-4 weldments.

This is due to the formation of grain boundary martensite in that region which increased the hardness of the region and in turn increasing the strength. The average ultimate strength and 0.2% proof strength for the ERNiCrMo-4 samples was 527 MPa and 338.7 MPa respectively. This may be reasoned out to the presence of major alloying elements such as W, Mo, Cr and minor alloying elements including Ti, V and Co exhibited strengthening effect to the matrix and made it stronger and tougher. Whereas for the ER2553 samples, the corresponding values were 459 MPa and 292.6 MPa (Table 4). The improvement in the weld strength could be attributed to the presence of ferrite which increases the hardness dramatically which in turn evident for such tensile behavior in case of ER2553 weldments. SEM fractographs (Fig. 17) divulged the fact that these weldments had undergone ductile mode of fracture owing to the presence of micro and macro-voids along with meagre dimpled facets which would have been coalesced.

3.3.3. Impact test and bend test

Charpy V notch test was performed on the weldments to investigate the response of the weldments towards sudden load. From the experimental trials, it was observed that the ER2553 weldments offered an average impact strength of 22 J whereas for the ERNiCrMo-4 weldments the corresponding value was 62 J (Table 4). The average impact toughness of both the weldments was found to be greater than the parent metal, AISI 430 whose impact toughness was 20 J. The studies showed that the average toughness of ER2553 weldments slightly impoverished which could be explained with the presence of skeletal delta ferrite and acicular ferrite in the fusion zone. However the dramatic increase in the impact toughness of ERNiCrMo-4 weldments shall be due to the presence complete austenitic structure and also reasoned out to the presence of principal strengthening elements. On observing the impact tested coupons, it is opined that the ER2553 weldments responded fairly to the impact energy by showing the complete rupture; whereas v-notch deformation was the classical feature for the ERNiCrMo-4 weldments, which in turn indicates that these weldments have responded well towards the impact loading. In addition, as stated above the average hardness value of the ER2553 weldments was higher than the average hardness of the ERNiCrMo-4 weldments, which is in concordance with the fact that higher the hardness, lower would be the toughness. SEM fractograph of ER2553 weldment showed the presence of tearing ridges and scarce voids along with the presence of secondary phases contributed for brittle mode of fracture (Fig. 18a). Whereas the ERNiCrMo-4 weldments was observed to have dome shaped facets with the presence of more voids which implied ductile mode of fracture (Fig. 18b).

To investigate the ductility and to ensure the soundness of the welded joints, the weldments were subjected to bend test. Root bend test was performed according to the ASTM: E 190-92 standard. The weldments employing the ERNiCrMo-4 filler did not reveal any type of cracking whereas the weldments of ER2553 showed significant cracking at weld lip of the SS430 interface and the data is represented in Table 4. This study addressed the joining of Inconel 718 and AISI 430 using ER2553 and ERNiCrMo-4 fillers by pulsed current GTA welding process. The structure – property relationships of these bimetallic joints were discussed in detail. The present study demonstrated that PCGTA welding is very effective and successful for joining dissimilar metals. Based on the structure – property information of the weldments, the present study recommends the use of ERNiCrMo-4 filler for joining Inconel 718 and AISI 430. This article presents the assessment of dissimilar weldments of Inconel 718 and AISI 430 using PCGTAW.

Table 4. Average mechanical properties of dissimilar weldments.

Test	Mechanical Property	Unit	ER2553 weldment	ERNiCrMo-4 weldment
Tensile Test	Max. Load	kN	9.8	9.09
	0.2% Proof Strength	MPa	292.6	338.7
	Ultimate tensile strength	MPa	459	527
	% Elongation at Break	(%)	8.87	8.03
	Fracture Zone	---	Parent Metal of AISI 430	Parent Metal of AISI 430
Impact Test	Impact Toughness	J	22	62
	Fracture appearance	---	Broken into two halves	V-notch deformation
Bend Test	Bending strength	MPa	65.68	74.63
	Visual Observation	---	Crack initiation at approx. 180˚ bend	Complete 180˚ bend was obtained without any surface irregularities

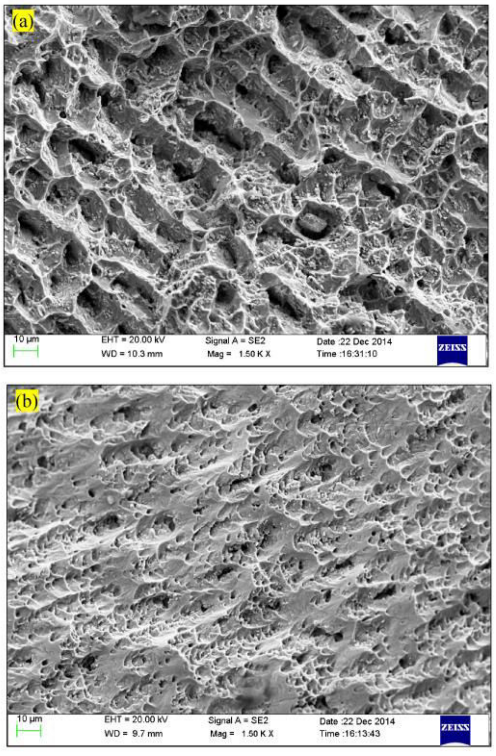

Fig. 18. SEM fractographs on the impact tested samples of (a) ER 2553 (b) ERNiCrMo-4 weldments.

4. Conclusions

The following conclusions were made from the current study.

1. Both filler wires ER 2553 and ERNiCrMo-4 can be used to successfully weld these metals using PCGTA welding.
2. Formation of Nb rich phases was observed while using both the filler wires. But there were no signs of solidification or liquation cracking.
3. Grain coarsening and formation of grain boundary martensite was observed in the HAZ of AISI 430 in both the cases.
4. The fusion zone of ER2553 experienced greater hardness than ERNiCrMo-4 due the formation of skeletal delta ferrite.
5. Tensile studies concluded that the joint strength is higher than the parent metal AISI 430. The tensile strength of both the fusion zones are greater than the base metal, AISI 430.
6. ERNiCrMo-4 weldment had higher impact toughness compared to the ER 2553 welds due the formation of complete austenitic microstructure in the weld zone.

Acknowledgements

The authors wish to convey their sincere thanks to Mr. Natarajan, Managing Director, Delta Wear Tech Engineers Pvt. Ltd., Chennai for providing the welding facilities to carry out experiments. Also the UTM facility provided to our University by DST under FIST scheme is gratefully acknowledged.

References

[1] International Stainless Steel forum. The ferritic solution. ISSF; 2007. http://www.worldstainless.org/news/show/34 dated 07.05.2015

[2] J.C. Lippold, D.J. Kotecki, Welding metallurgy and weldability of stainless steels. New Jersey, Wiley-Interscience, 2005.
[3] R. Castro, J.J. De Cadenet, London, Welding Metallurgy of Stainless and Heat Resisting Steels, Cambridge University Press, 1974.
[4] H.W. Hayden, S. Floreen, Metall. Trans. 1 (1972) 1950.
[5] R.N. Wright, J.R. Wood, Metall. Trans. 8A (1977) 1977.
[6] S. Antilla, H.-P. Heikkinen, Structural Applications of Ferritic Stainless Steels. Finland: Outokumpu Stainless Oy Tornio Research Centre, 2014.
[7] J. Sedriks, Corrosion of Stainless Steels. New Jersey: Wiley-Interscience, 1996.
[8] J.N. DuPont, J.C. Lippold, S.D. Kiser, Welding metallurgy and Weldability of Nickel base alloys, New Jersey: John Wiley & Sons Inc., 2009.
[9] A. Odabasi, N. Unlu, G. Goller, M.N. Eruslu, The Minerals, Metals & Materials Society, 2010.
[10] G.D.J. Ram, A.V. Reddy, K.P. Rao, G.M. Reddy, Sci. Technol. Weld. Joining 9(5) (2004) 390.
[11] S.G.K. Manikandan, D. Sivakumar, K. Prasad Rao, M. Kamaraj, Mater. Charact. 100 (2015) 192.
[12] K.D. Ramkumar, S.D. Patel, S.S. Praveen, D.J. Choudhury, P. Prabaharan, N. Arivazhagan, M.A. Xavior, Mater. Des. 62 (2014) 175.
[13] C. Radhakrishna, K.P. Rao, J. Mater. Sci. 32(8) (1997) 1977.
[14] K.D. Ramkumar, V. Joshi, S. Pandit, M. Agrawal, O.S. Kumar, S. Periwal, M. Manikandan, N. Arivazhagan, Mater. Des. 64 (2014) 775.
[15] K.D. Ramkumar, P. Mithilesh, D. Varun, A. Reddy, N. Arivazhagan, S. Narayanan, K.G. Kumar. ISIJ International, 54 (2013) 900.
[16] E. Farahani, M. Shamanian, F. Ashrafizadeh, Int. J. Manuf. Mater. Sci. 02 (2012) 1.
[17] F.B. Pickering, American Society for Metals; 1979.
[18] S. Kou. Welding Metallurgy. New Jersey: Wiley Publication; 1987.
[19] M. Alizadeh, S.P.H. Marashi, M. Pouranvari, Mater. Des. 56 (2013) 258.
[20] V.V. Satyanarayana, G.M. Reddy, T. Mohandas, J. Mat. Proc. Tech. 160 (2005) 128.
[21] M. Shamanian, A. Mortezaie, Int. J. Pressure Vessels Piping 116 (2014) 37.
[22] M. Sireesha, S. Albert, V Shankar, S. Sundaresan, J. Nucl. Mater. 279 (2000) 65.
[23] C.-C. Hsieh, D.-Y. Lin, W. Wu, Met. Mater. Int. 13 (2008) 643.
[24] R.L. Bodnar, S.S. Hansen, Metall. Mater. Trans. A, 25A (1994) 665.
[25] S. Kou, Y. Le, Weld. Res. Suppl. (1986) 305.
[26] C.-C. Hsieh, D.-Y. Lin, M.-C. Chen, W. Wu, Mater. Trans. 18 (2007) 2898.